Supporting Information for "The Increasing Efficiency of the Poleward Energy Transport into the Arctic in a Warming Climate"

Christopher J. Cardinale[1], and Brian E. J. Rose[1]

[1]Department of Atmospheric and Environmental Sciences, University at Albany, State University of New York, Albany, New York

Contents of this file

1. Figures S1 to S4

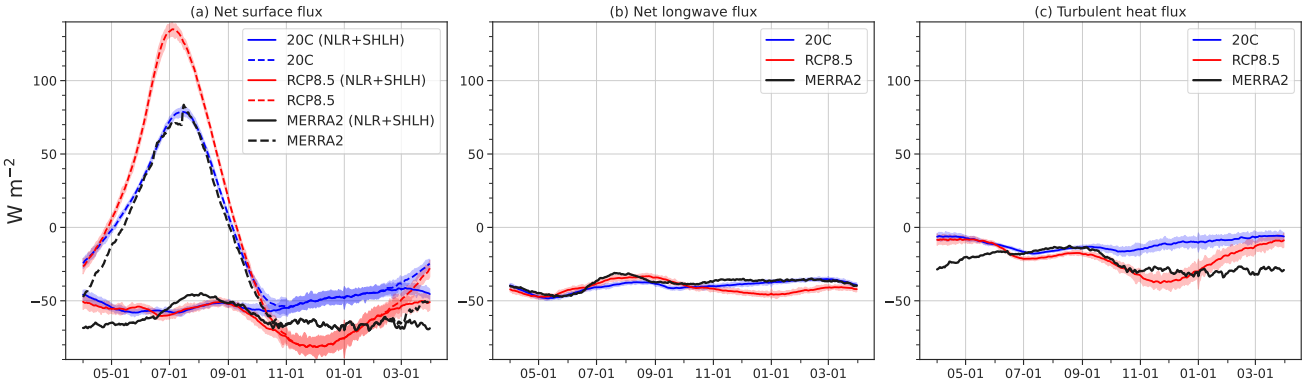

Figure S1. Mean annual cycle of the polar cap–averaged (a) net surface flux (NSF; dashed; including net absorbed shortwave radiation) and contributions to the NSF from the combined net longwave and turbulent heat fluxes (NLR+SHLH; solid; not including shortwave radiation), (b) net longwave flux, and (c) turbulent heat fluxes (SHLH). All panels are positive down (atmosphere to surface) in units of W m^{-2}, and comparing the 20C (blue) and RCP8.5 (red) simulations from the CESM-LE to the MERRA-2 (black). Shading indicates the ensemble 5th–95th percentile range.

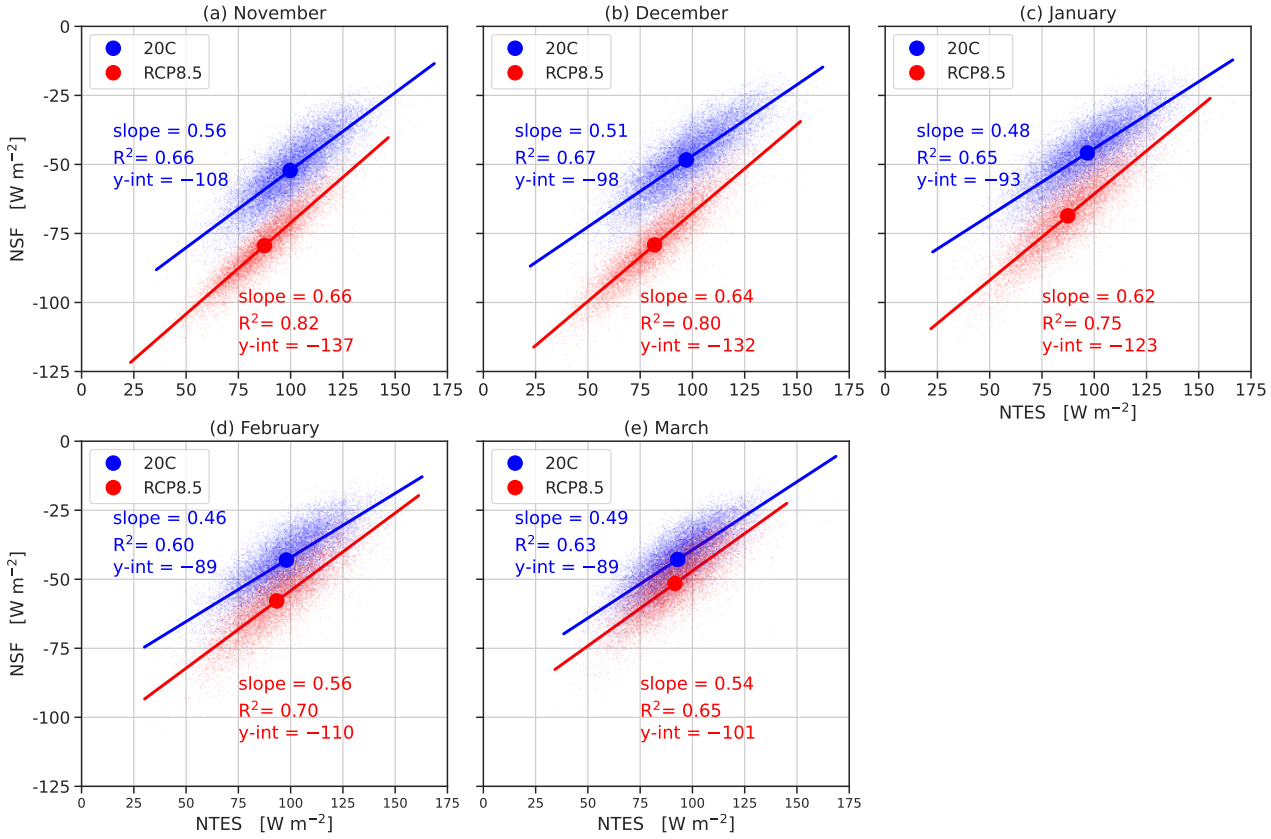

Figure S2. Daily mean NSF against NTES during (a)–(e) each winter month (November–March) in the 20C (blue; $\mathrm{W\,m^{-2}}$) and RCP8.5 (red; $\mathrm{W\,m^{-2}}$) runs of the CESM-LE. For each ensemble and month, the linear regression (solid lines), climatological mean (large circles), slope, coefficient of determination ($\mathrm{R^2}$), and y-intercept ($\mathrm{W\,m^{-2}}$) are shown. Grouping by month reduces the impact of the seasonal cycle on the slopes of the regression lines.

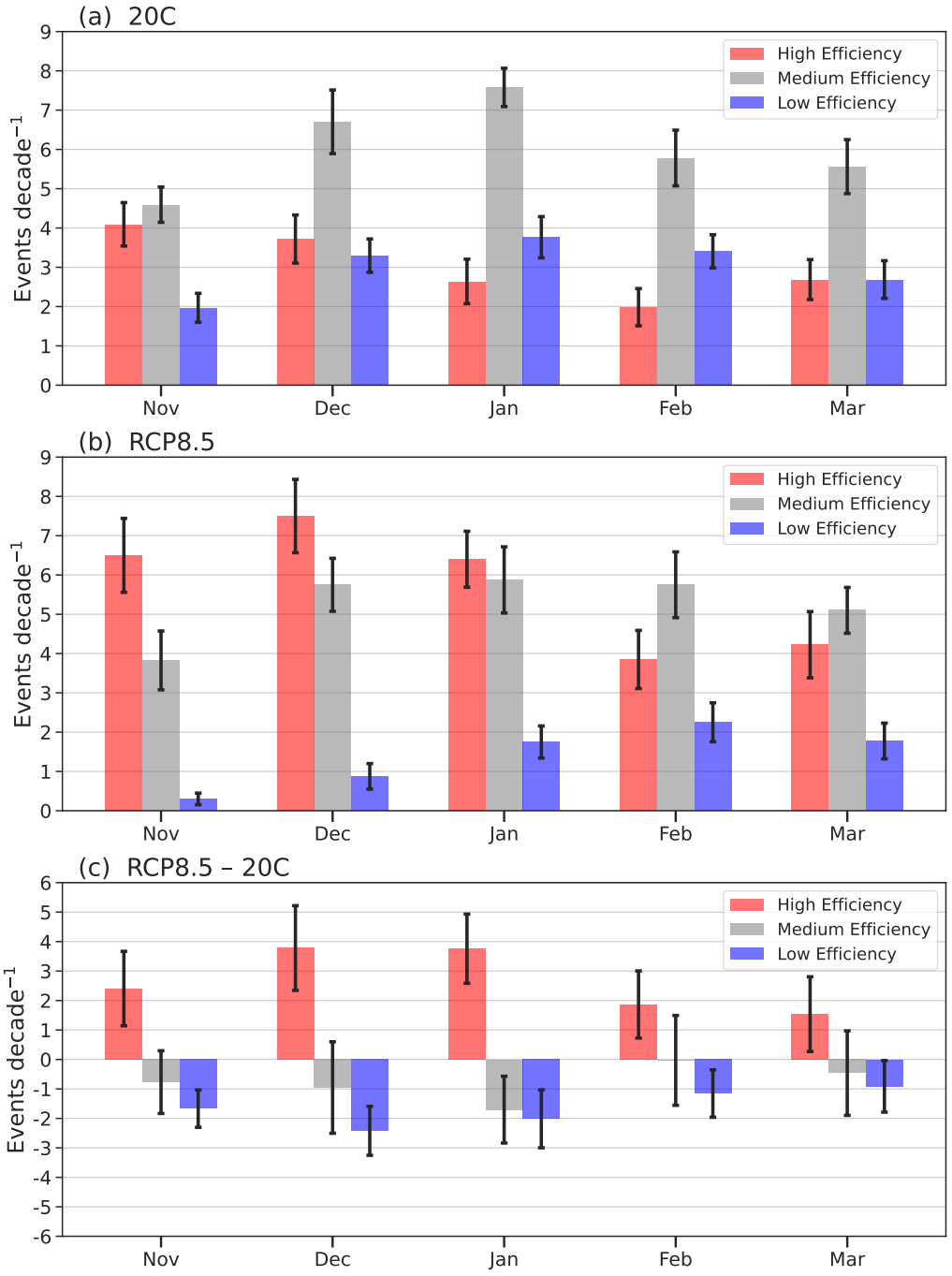

Figure S3. Average number of high (red), medium (gray), and low-efficiency (blue) events per decade for each winter month in the (a) 20C and (b) RCP8.5 runs of the CESM-LE. (c) shows the difference (RCP8.5 – 20C). Vertical lines indicate the 95% confidence interval.

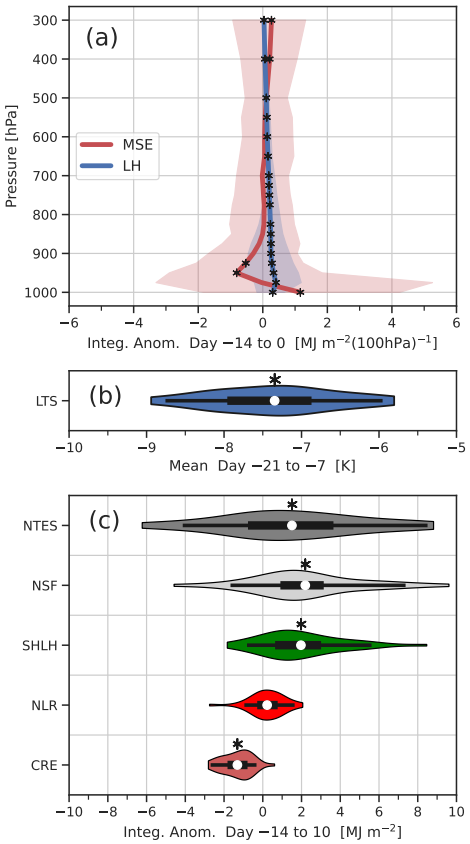

Figure S4. Composite of the change (RCP8.5 − 20C) in the (a) time-integrated anomalous local moist static energy (MSE; red) and latent heat (LH; blue) flux convergence [MJ m^{-2} (100 hPa)$^{-1}$] from day −14 to 0 in F_{trop} events (combined high, medium, and low-efficiency events). (b) shows the change in mean lower-tropospheric stability (LTS; blue; K) between days −21 and −7. (c) shows the change in time-integrated anomalies in the net tropospheric energy source (NTES; gray; MJ m^{-2}), net surface flux (NSF; light gray; MJ m^{-2}), combined sensible and latent surface turbulent heat fluxes (SHLH; green, MJ m^{-2}), net longwave radiation (red; MJ m^{-2}), and surface cloud radiative effect (CRE; MJ m^{-2}) from day −14 to −10. Violin plots follow the same convention as in Fig. 1. The shading in (a) indicates the ensemble 5th–95th percentile range. Asterisks indicate ensemble means statistically different from low-efficiency events at 95% confidence.